

Special
Collection

One, Two Three – Phosphaalkene Decoration Tailoring Solubility and Electronic Properties of Truxene-Based Electron Acceptors

Muhammad Anwar Shameem^{+, [a]} Jordann A. L. Wells^{+, [a]} Arvind K. Gupta,^[a] and Andreas Orthaber^{*[a]}

Abstract: We report the functionalization and deplanarization of truxenes using pnictaalkene fragments. Selective introduction of one, two, or three Mes^{*}-Pn fragments provides up to three fully reversible reductions based on the Pn=C fragments. The incorporation of the unsaturated heteroelement fragment as well as the contortion of the truxene core result in significantly red-shifted absorption spectra and interesting opto-electronic properties which are studied by electrochem-

istry and spectro-electrochemistry. Incorporation of arsaalkene (As=C) motifs gives significantly milder reduction potentials and red-shifted absorption, while phosphaalkene decorated truxene **P3** can be functionalized using Au(I)Cl coordination. Furthermore, solubility is markedly increased upon incorporation of the Pn-Mes^{*} fragments which renders these materials suitable for solution processing.

Introduction

Polyaromatic hydrocarbons (PAHs) are highly stable planar structures mainly composed of sp² carbon atoms decorated with relatively few hydrogen atoms. Incorporating heteroatoms or heterocycles able to accept or donate electron density results in unique electronic and photophysical properties.^[1] In recent years, contorted PAHs, that is, extended conjugated aromatic systems that deviate from ideal planarity, have received increasing attention due to their fascinating electronic properties^[2] with a particular focus on truxene fragments as versatile electron acceptors.^[3]

Like other main group elements (e.g., S, O, N, etc.), inclusion of heavy group 15 elements in PAH has a marked influence on their electronic properties.^[4] The incorporation of group 15 centers in PAH has mainly been limited to saturated heteroatoms, for example phenyl phosphine chalcogenide,^[5] phospholes,^[6] phosphaphenalenenes,^[7] etc. In contrast, a few

reports of low-coordinate phosphorus in unsaturated organic compounds and PAHs have already had a significant impact on the field of organic electronics.^[8] In particular, pnictaalkene moieties have been shown to significantly stabilize the LUMO levels of extended pi-systems and give rise to interesting opto-electronic properties.^[9] Within the last decade, thermally stable P-centred phosphaalkenyl radical mono- and dianions based on PAH fragments (fluorene, indenofluorene), and a carbene stabilized diphosphabutadiene radical cation have been isolated, illustrating the strategic potential of (heavy) pnictogen incorporation into PAH fragments for opto-electronic applications.^[10] In this work, we present de-planarization and electronic tuning of the truxene core, extending the conjugated system by exocyclic phospha- and arsaalkenes. The resulting optical and electronic properties are largely dictated by the pnictaalkene moiety, which gives rise to pronounced acceptor character and stabilized radical anions (Figure 1).

Results and Discussion

Truxene is a polycyclic fragment of C₆₀-fullerenes, consisting of four C₆ rings and three C₅ rings. The parent compound (**H₆Trux**) and its oxidized derivatives feature a planar truxene core and exhibit poor solubility in commonly used laboratory solvents. Alkylation at the methylene positions circumvents this issue, while maintaining the planarity in the system. In an attempt to introduce two-coordinate phosphorus fragments, that is, targeting triphosphaalkene **P3**, the truxenide trianion was exposed to excess Mes^{*}PCl₂ in THF at −78 °C, followed by DBU addition (Scheme 1a). Following chromatographic work-up, **P3** was obtained as a dark red solid in yields of up to 45% (based on **H₆Trux**). The ¹H NMR spectrum suggests a fully symmetric conformation for **P3**, exhibiting a single resonance for the Mes^{*}

[a] Dr. M. A. Shameem, Dr. J. A. L. Wells, Dr. A. K. Gupta, Dr. A. Orthaber
Synthetic Molecular Chemistry, Department of Chemistry
Ångström Laboratory
Uppsala University
Box 523, 75120 Uppsala (Sweden)
E-mail: andreas.orthaber@mail.uu.se
Homepage: <http://www.kemi.uu.se/angstrom/research/synthetic-molecular-chemistry/research-groups/orthaber-group>

[*] These authors contributed equally to this work.

Supporting information for this article is available on the WWW under <https://doi.org/10.1002/chem.202300563>

Part of a Special Collection on the p-block elements.

© 2023 The Authors. Chemistry - A European Journal published by Wiley-VCH GmbH. This is an open access article under the terms of the Creative Commons Attribution Non-Commercial NoDerivs License, which permits use and distribution in any medium, provided the original work is properly cited, the use is non-commercial and no modifications or adaptations are made.

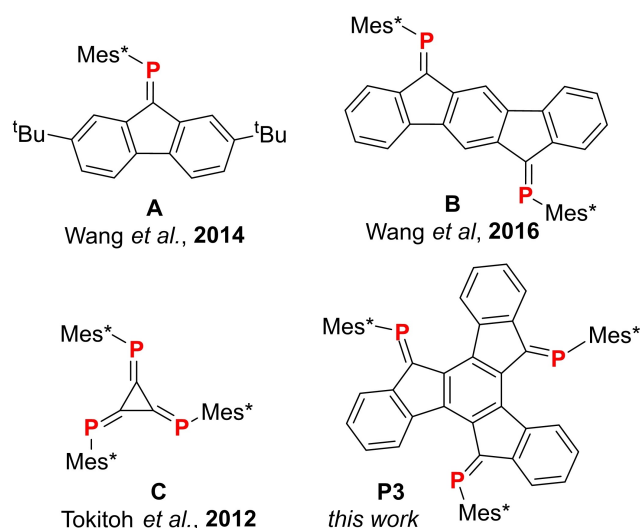
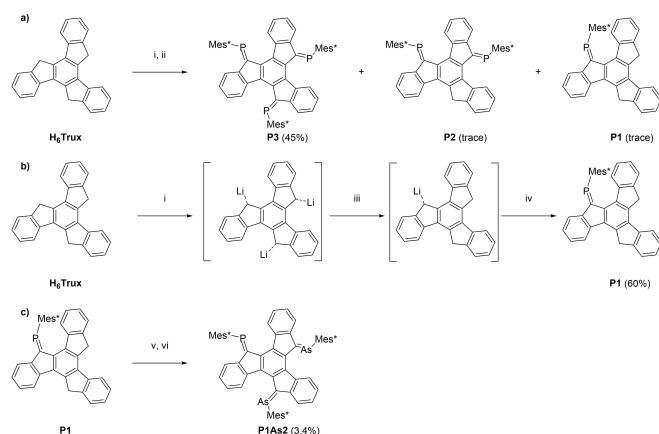


Figure 1. Phosphaalkenes and their radical anions within extended π -conjugated PAHs. **A&B:** planar fluorenyl and extended fluorenyl based (di)phosphaalkene systems.^[10a,b,11] **C:** Triphospha[3]radialene.^[12] *This work:* Non-planar truxene based phosphaa-(arsa-)alkene systems.



Scheme 1. Synthesis of **P3**, **P2**, **P1**, **P1As2**. i) 3 equiv. *n*-BuLi -78°C THF. (ii) 4 equiv. $\text{Mes}^*\text{P-Cl}_2$ 1 h then xs. DBU, THF. (iii) 2 equiv. H_2O , THF. (iv) 2 equiv. $\text{Mes}^*\text{P-Cl}_2$ 1 h then xs. DBU, THF. (v) 2.2 equiv. *n*-BuLi -78°C THF. (vi) 3 equiv. $\text{Mes}^*\text{As-Cl}_2$ 1 h then xs. DBU, THF.

aryl *meta* protons ($\delta = 7.50$ ppm), as well as for the *ortho* and *para tert-butyl* protons ($\delta = 1.43$ ppm). The four aryl protons of the truxene core range 9.15 – 5.29 ppm with the expected multiplicity; the highly deshielded resonance at 9.15 ppm was ascribed to the β proton proximal to the phosphaaalkene (Figure 2). The highly symmetrical conformation of **P3** is supported by the $^{31}\text{P}\{^1\text{H}\}$ NMR spectrum with a single resonance at 259.6 ppm, which is consistent with other “fluorenyl-like” phosphaaalkenes.^[11,13] Besides 4,5,6-triphospha[3]radialene **C** (Figure 1),^[12] **P3** is the only other example which incorporates more than two phosphaaalkene units into a single conjugated organic fragment.

Two further compounds, characterised as orange-red di-phosphaalkene **P2** and orange monophosphaalkene **P1** (Scheme 1a), were isolated after chromatographic work-up, likely

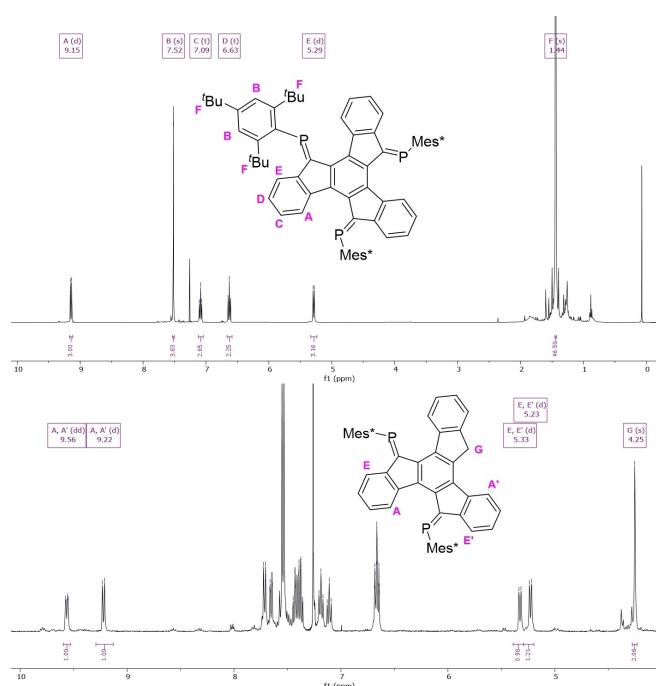


Figure 2. *Top:* Representative ^1H NMR (CDCl_3 , 400 MHz) spectrum of **P3** illustrating the symmetric nature of the trisubstituted product and the deshielding and shielding effects on protons A and E, respectively. *Bottom:* Selected region of the ^1H NMR spectrum of **P2** showing the deshielded and shielded signals (A, A' and E, E') as well as the unsubstituted methylene bridge (G).

formed from the incomplete formation of the truxenide trianion or partial hydrolysis. Direct mono- and dilithiation of truxene was unsuccessful due to its poor solubility compared to the anionic intermediates. However, the targeted synthesis of **P1** was achieved in good yields (ca. 60%) by the protonation of trilithiated truxenes with two equivalents of water, followed by addition of $\text{Mes}^*\text{P-Cl}_2$ and HCl elimination with excess DBU (Scheme 1b). The solubility of all three derivatives is considerably increased compared to parent **H₆Trux**, and derivatives **P2** and **P3** show significant solubility in alkanes (e.g., pentane, hexane). Attempts to synthesise **P2** in a manner analogous to **P1** were unsuccessful. The ^1H NMR spectrum of **P2** contains several resonances consistent with the low symmetry of the molecule. Two deshielded doublet resonances for the aryl protons β to the phosphaaalkenes can be observed at 9.57 ppm ($^3J_{\text{HH}} \approx 8.0$ Hz) and 9.33 ppm ($^3J_{\text{HH}} \approx 8.0$ Hz), which suggests a contortion in the planarity of the truxene core. Two broad singlets of equal integration at 7.55 and 7.54 ppm, can be ascribed to the Mes^* *meta* aromatic protons, and a broad singlet at 4.24 ppm was assigned to the unsubstituted truxene core methylene protons. The ^{31}P NMR spectrum of **P2** contains two singlets at 265.4 and 259.5 ppm which also point towards significant differences in the P-environments. The ^1H NMR spectrum of monophosphaalkene **P1** exhibits a characteristic deshielded pseudo-triplet resonance at 9.8 ppm, due to a rare example of through-space $\text{P} \cdots \text{H}$ coupling ($J_{\text{PH}} \approx 8.0$ Hz), which resolves to a doublet ($^3J_{\text{HH}} \approx 7.8$ Hz) in the $^1\text{H}\{-^{31}\text{P}\}$ NMR

spectrum. The triplet was assigned to the aryl proton proximal to the P centre. Other noteworthy resonances are the broad singlets of the truxene core methylene protons, with chemical shifts of 4.30 and 4.20 ppm. The ^{31}P NMR spectrum of **P1** exhibits a deshielded resonance at 269.8 ppm. Having established a reliable route towards **P1**, we were also able to obtain the mixed pnictaalkene species **P1As2** using a sequential process in very low yields. The compound is characterized by a single ^{31}P resonance (262 ppm), however the reduced symmetry of this system is clearly reflected in its ^1H spectrum.

Single crystals were obtained from slow evaporation of pentane solutions of **P2**, and by diffusion of pentane into concentrated toluene solutions of **P1**. The solid-state structure of **P1** shows that the truxene core is significantly contorted (Figure 3). The phosphalkene moiety is twisted out by $61.6(1)^\circ$ of a near co-planar arrangement of two indene arms. The third unsubstituted indene shows another contortion towards these near coplanar indene arms (angle between least squares planes of $22.54(3)^\circ$) further minimizing steric interactions with the Mes* substituent. Notably the P–C bond has a *cis* configuration, that is, facing the central phenyl ring.^[14] While the P=C bond is in the expected range ($1.695(2)$ Å) the C–P=C angle is significantly widened to $111.2(1)^\circ$. These structural differences could also explain why the pronounced through space ^{31}P – ^1H coupling is exclusive to this derivative (see above). The packing shows π – π stacking of two molecules related by inversion symmetry, giving rise to centroid-centroid distances of ca. 3.7 Å. In the solid-state structure of **P2**, the unsubstituted indene remains coplanar with the central phenyl ring, while the two flanking phosphorylated indenenes twist out of the plane to give a propeller-like conformation. Notably, the P–C bonds have a *trans*-configuration, that is, the Mes* groups pointed towards

the outer phenyl rings. The P1–C1 and P2–C17 bond distances are similar to those in **P1** and within the expected range for P–C double bonds at $1.696(2)$ and $1.694(2)$ Å, respectively. The C–P–C angles range $103.7(1)^\circ$ to $104.0(1)^\circ$, which is comparable to related phosphalkenes,^[9a] however significantly smaller than that in **P1**. No π – π interactions were observed for **P2** in the solid-state packing.

In lieu of the structure of **P3**, we were able to obtain a trinuclear gold(I) complex, **P3(AuCl)₃** by reaction of **P3** with [AuCl(tht)] (tht = tetrahydrothiophene) in DCM (Scheme 2). The ^1H NMR spectrum of **P3(AuCl)₃** is comparable to that of highly symmetric **P3**, while the ^{31}P NMR spectrum contains a single broad resonance at 185.9 ppm, consistent with metal coordination to a phosphalkene. Single crystals suitable for X-ray diffraction studies were obtained by slow evaporation from DCM solutions. Gold complex **P3(AuCl)₃** displays a notable distortion from planarity similar to the propeller arrangement observed in **2**. Intermolecular π -stacking to a dimeric motif occurs also in **P3(AuCl)₃**, where two molecules stack on top of each other in a eclipsed arrangement giving rise to a small cavity with a moderate centroid-centroid distance of 4.17 Å of the central truxene hexagon (Figure 3). Theoretical studies of two different conformations of the truxene core, that is, *up,up,up*-**P3** (as observed **P3(AuCl)₃**) and the less symmetric *up,up,down*-**P3**^[15] show that the former is energetically favourable by ca. 6.5 kJ/mol clearly indicating that subtle changes and intramolecular interactions can influence the arrangement of the truxene core. Low temperature NMR studies are consistent with the symmetric *up,up,up*-**P3** conformation or rapid interconversion of these isomers. Rapid interconversion of isomers is most likely, however we have been unable to experimentally verify this assumption.

The UV-vis absorption spectra of **P3**, **P2**, and **P1** and **P1As2** measured in DCM are shown in Figure 4, and the maximum absorption wavelengths were summarized in Table 1. Notably, phosphalkene **P1** exhibits a substantially red-shifted absorp-

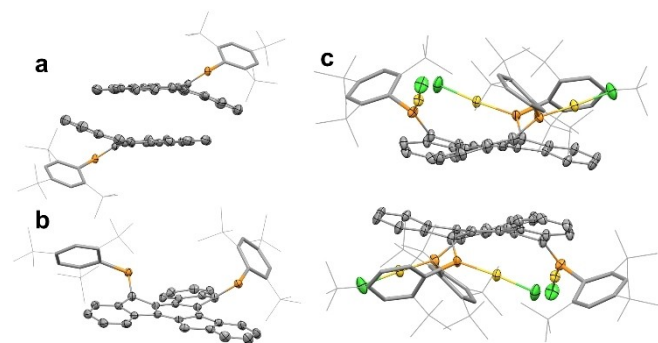
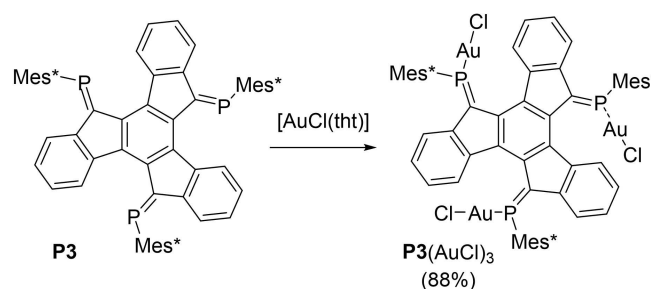


Figure 3. Solid-state structures of monophosphalkene **P1** showing the π – π stacking of two symmetry related units (a), diphosphalkene **P2** (b), as well as trinuclear gold complex **P3(AuCl)₃** showing the cavity formed by π – π stacking of two symmetry equivalent molecules (c). Further crystallographic data are summarized in the Supporting Information.



Scheme 2. Synthesis of trinuclear gold complex **P3(AuCl)₃** from **P3**. Conditions: DCM, r.t. 2 h.

Table 1. Comparison of the optical and electronic properties of **H₆Trux**, **P1**, **P2**, **P3**, and **P1As2**.

Entry	H₆Trux	P1	P2	P3	P1As2
λ_{max} [nm] ^[a]	298, 291	428, 317	435, 325	452, 390, 330	468, 419, 339
$E_{1/2}$ [V] ^[b]	–2.59 (irr)	–1.92	–1.77, –2.2*	–1.89, –2.23, –2.67	–1.75, –2.15, –2.68

[a] DCM; [b] THF/[nBu₄N][PF₆] $v = 100$ mV s^{–1}; * collected in DCM.

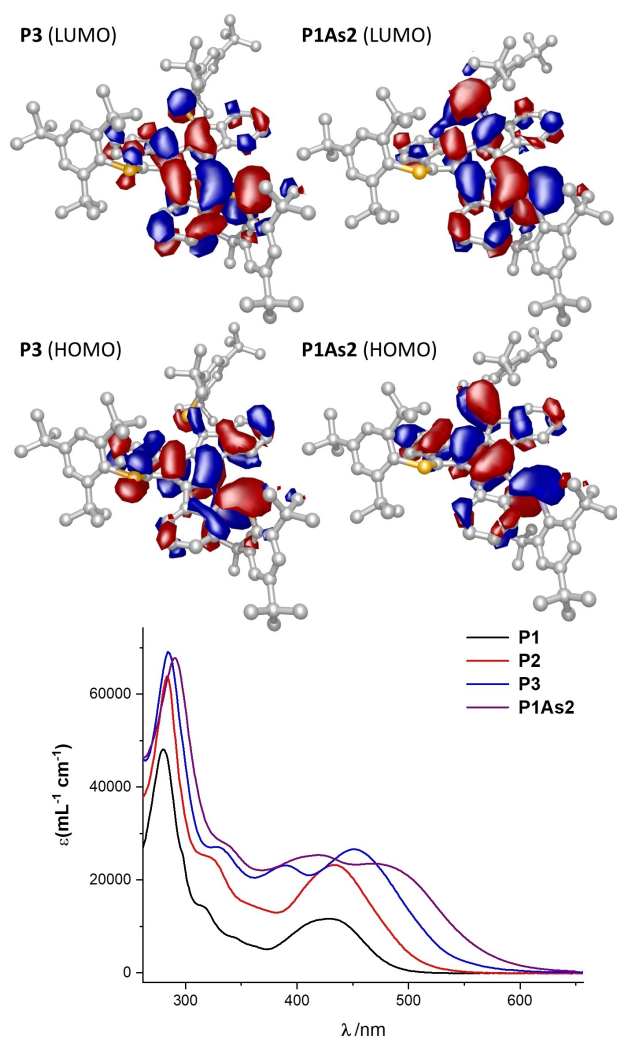


Figure 4. Top: Frontier molecular orbitals of the **P3** and **P1As2** derivatives illustrating the involvement of the P=C and As=C units (Calculated at the B3LYP/6-311G** level of theory). Bottom: UV-Vis spectra of **P1**, **P2**, **P3** and **P1As2** in DCM.

tion maximum (π - π^* electronic transition), with λ_{\max} of 428 nm compared to 298 nm in **H₆Trux**, that is, 154 nm, which can be explained by the integration of acceptor units (i.e., phosphaaalkenes) into the conjugated truxene core, which induces structural changes in the supporting truxene core and considerably decreases the LUMO levels. This is also significantly red-shifted compared to the fluorenylidene phosphaaalkene (368 nm) reported earlier.^[13] Increasing the number of phosphaaalkenes results in a slight red-shift of 7 nm for **P2** (with an almost two-fold increase of absorptivity) and a more notable red-shift of 24 nm in **P3**. This suggests only minor communication between the two phosphaaalkene centres in **P2**, while cooperative effects are more pronounced in **P3**. The mixed **P1As2** derivative shows a clearly distinct UV/vis spectrum where the low energy band splits into two maxima at 419 nm and 468 nm. The further red-shift (16 nm compared to **P3**) is in line with an expected lowering of HOMO–LUMO splitting by means of arsaalkene incorporation. (Figure 4)

The redox properties of compounds **P1**, **P2**, and **P3** as well as **P1As2** were investigated by cyclic voltammetry in THF/ $[n\text{Bu}_4\text{N}][\text{PF}_6]$ (Table 1). The cyclic voltammogram of **P3** shows three fully reversible one-electron redox events at -1.89 , -2.23 , and -2.67 V versus Fc/Fc^+ (Figure 5). The cyclic voltammogram of monophosphaaalkene **P1** shows a single reversible redox event at -1.92 V, while **P2** gives a clear reversible reduction at -1.77 V and a second reduction process around -2.25 V that is partially obscured. In line with the irreversible reduction of **H₆Trux**, the redox events in **P1–P3** can be attributed to the phosphaaalkene/phosphaaalkenyl radical couple. The potentials are less negative when compared to fluorenyl phosphaaalkene **A** (-1.99 V versus Fc/Fc^+)^[13] illustrating the extended conjugation. Notably the peak separation in diphosphaaalkene **B** ($E_{1/2} = -1.72$ V and -2.35 V versus Ag/AgNO_3 mV// -1.87 V and -2.50 V versus Fc/Fc^+) is significantly larger (ca. 600 mV) compared to that in **P2** (ca. 450 mV) and **P3** ($\text{P3}^- \rightarrow \text{P3}^{2-}$ 340 mV and $\text{P3}^{2-} \rightarrow \text{P3}^{3-}$ 440 mV). The smaller difference in potential between redox events in our truxene systems allows the observation of three reductions within the same potential

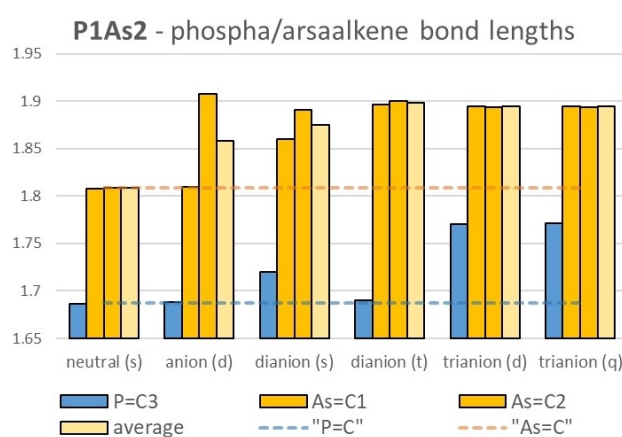
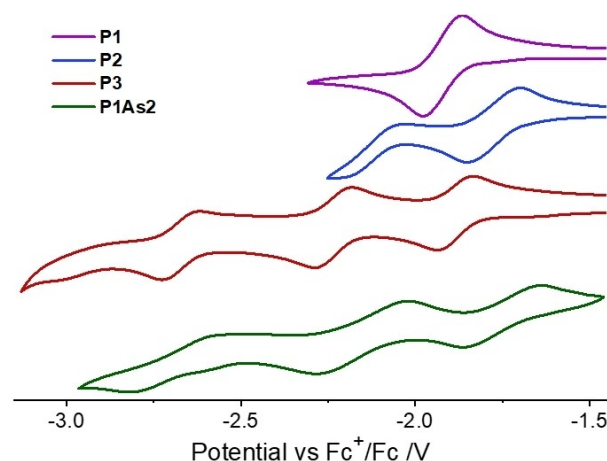


Figure 5. Top: Cyclic voltammograms of **P1**, **P2**, **P3** and **P1As2**. Potentials are reported versus Fc^+/Fc . Conditions: 0.1 M $[\text{nBu}_4\text{N}][\text{PF}_6]$ in THF (*or DCM), scan rate 100 mV sec^{-1} . Bottom: Changes of phosphaaalkene and arsaalkene bond lengths upon reduction. Dashed lines indicate ideal double bond lengths for phosphaaalkene-c and arsaalkene. Geometries are optimized at the B3LYP/6-311G** level of theory.

window.^[10b] Interestingly, triphospha-[3]-radialene **C**, could only undergo two consecutive one electron reductions ($E_{1/2} = -1.55$ V and -2.62 V vs. Fc^+/Fc) giving the dianion C^{2-} .^[16] The stark difference can be rationalized by the significantly smaller and completely coplanar organic core of **C**. The mixed **P1As2** derivative illustrates the capacity of heavier pnictogen substitution to modulate PAH electronics. Three reversible reductions, reminiscent to those of **P3**, are observed of which two are shifted to milder potentials ($E_{1/2} = -1.7$ and -2.1 V vs. Fc^+/Fc) while the third is barely affected (2.7 V vs. Fc^+/Fc) showing the selective tuning opportunities of the truxene motif. Peak separations are approx. 400 mV ($\text{PAs2} \rightarrow \text{PAs2}^-$, $\text{PAs2}^- \rightarrow \text{PAs2}^{2-}$) and 600 mV ($\text{PAs2}^{2-} \rightarrow \text{PAs2}^{3-}$). Together with the theoretical calculations (see below), this indicates that the ultimate reduction process is based on the $\text{P}=\text{C}$ fragment, while the former two are $\text{As}=\text{C}$ based, that is, effectively stabilizing the lowest unoccupied molecular orbitals.

As a representative example, spectro-electrochemistry of **P3** was performed in order to gain further information about the reduced species (for details see Supporting Information). Upon reduction at -1.8 V a clean conversion to radical anion P3^- was observed, which shows a decreased absorption of the bands around 390 nm (corresponding to a $\pi-\pi^*$ transition of the heterofulvenoid) and a rising band around 600 nm (corresponding to $\pi-\pi^*$ transitions from reduced to non-reduced heterofulvenoid cores). In dianion P3^{2-} , obtained by reduction at -2.2 V, a further increase and appearance of a further shoulder of the low energy bands indicates increased charge transfer character. Upon full reduction (at -2.7 V), the low energy bands become less intense, which is in line with the fully reduced triphosphaalkenyl state. DFT calculations of P3^{n-} (for $n=1, 2$ and 3) show a sequential increase of the average phosphalkene distance upon reduction from $d(\text{P}=\text{C})_{\text{avg.}} = 1.688$ Å in **P3** to 1.771 Å in P3^{3-} . This clearly supports population of antibonding orbitals with pronounced phosphalkene contributions. Singlet and triplet P3^{2-} show a moderate and strong localization of the spin density over three ($d(\text{P}=\text{C}) = 1.759, 1.725$, and 1.711 Å) and two ($d(\text{P}=\text{C}) = 1.771, 1.769$, and 1.691 Å) phosphalkene units, while trianion P3^{3-} shows full delocalization and elongation of all three phosphalkene units (P3^{3-} - (doublet) $d(\text{P}=\text{C}) = 1.771$ Å and P3^{3-} - (quartet) $d(\text{P}=\text{C}) = 1.778, 1.779$, and 1.776 Å). As expected, the initial formation of the P1As2^- anion localizes the additional electron density on mainly one arsaalkene motif (elongating the $\text{As}=\text{C}$ distances from 1.808 Å (average) to 1.907 Å and 1.809 Å), while the $\text{P}=\text{C}$ bond remains at 1.688 Å, close to the initial bond length. Similarly, the second reduction populates antibonding orbitals incorporating both arsaalkene units, giving a $d(\text{As}=\text{C})_{\text{avg.}}$ of 1.875 (singlet) and 1.898 (triplet) Å, while only the third reduction gives a noticeable increase of the $\text{P}=\text{C}$ bond length for P1As2^{n-} (m): 1.686 Å ($n=0, m=s$), 1.688 Å ($n=1, m=d$), 1.720 Å ($n=2, m=s$), 1.691 Å ($n=2, m=t$), 1.770 Å ($n=3, m=d$), 1.771 Å ($n=3, q$). Notably there is a further elongation of the $\text{As}=\text{C}$ bond in the fully reduced species ($d(\text{As}=\text{C})_{\text{avg.}} = 1.895$ Å, $n=3, m=d$ and q).

Conclusions

In conclusion, we have reported novel polyaromatic-pnictaalkenes based on a highly contorted truxene motif. Folding and intermolecular $\pi-\pi$ interactions are strongly dependent on the number of functionalized methylene bridges as well as metal coordination of the pnictogen centre. The nature and number of introduced pnictogen centres also enables up to three highly tuneable and fully reversible reductions, making these compounds interesting for applications as non-fullerene acceptor materials. Future studies will investigate peripheral truxene substitution as well as additional mixed pnictaalkene derivatives.

Experimental Section

All manipulations were carried out under an inert atmosphere using Schlenk techniques or a glove box.^[17] Notably, the reported products are stable as solids under ambient conditions and can be purified using standard chromatographic conditions.

Deposition Number(s) 2237957 (for **P1**), 2237959 (for **P2**), 2237960 (for **P3**(AuCl)₃) contain(s) the supplementary crystallographic data for this paper. These data are provided free of charge by the joint Cambridge Crystallographic Data Centre and Fachinformationszentrum Karlsruhe Access Structures service.

Synthesis of P3: To a stirring pale-yellow suspension of TruxH_6 (1.0 g, 2.92 mmol) in THF was added $n\text{-BuLi}$ (2.5 M, 10.25 mmol), providing an orange red solution. The reaction mixture was allowed to stir at room temperature for an hour, then cooled to -78°C and Mes^*PCl_2 (3.75 g, 10.8 mmol) in THF (10 cm^3) was added and slowly allowed to reach r.t. overnight. DBU (2.2 cm^3 , 14.2 mmol) was added in one portion to slowly give a deep red solution which was continued to stir for 1.5 h. The crude reaction mixture was subjected to column chromatography with a pentane to pentane/toluene (2:98) gradient giving **P3** as the major product (1.5 gr., ca. 45%) with a single ^{31}P resonance (162 MHz, CDCl_3): 259.6 (s). Minor amounts of **P1** (^{31}P NMR: 270.1; s) and **P2** (^{31}P NMR: 265.4 (s), 259.6 (s)) have also been isolated from this reaction.

Acknowledgements

The authors would like thank the Swedish Research Council (2021-03658 and 2017-03727), the Olle-Engkvist foundation, Carl-Trygger foundation for financial contribution. Computational resources are provided by UPPMAX (snic2022/5-194 and snic2019/3-491).

Conflict of Interest

The authors declare no conflict of interest.

Data Availability Statement

The data that support the findings of this study are available in the supplementary material of this article.

Keywords: arsaalkene · contorted aromatics · organic radical · phosphaaalkene π -conjugation

- [1] R. Rieger, K. Müllen, *J. Phys. Org. Chem.* **2010**, *23*, 315–325.
- [2] a) X. Yang, F. Rominger, M. Mastalerz, *Angew. Chem. Int. Ed.* **2019**, *58*, 17577–17582; *Angew. Chem.* **2019**, *131*, 17741–17746; b) X. Yang, M. Hoffmann, F. Rominger, T. Kirschbaum, A. Dreuw, M. Mastalerz, *Angew. Chem. Int. Ed.* **2019**, *58*, 10650–10654; *Angew. Chem.* **2019**, *131*, 10760–10764.
- [3] G. Zhang, V. Lami, F. Rominger, Y. Vaynzof, M. Mastalerz, *Angew. Chem. Int. Ed.* **2016**, *55*, 3977–3981; *Angew. Chem.* **2016**, *128*, 4045–4049.
- [4] a) M. Hirai, N. Tanaka, M. Sakai, S. Yamaguchi, *Chem. Rev.* **2019**, *119*, 8291–8331; b) M. Stolar, T. Baumgartner, *Chem. Asian J.* **2014**, *9*, 1212–1225; c) R. Szucs, P. A. Bouit, L. Nyulaszi, M. Hissler, *ChemPhysChem* **2017**, *18*, 2618–2630; d) J. D. R. Ascherl, C. Neiß, A. Vogel, J. Graf, F. Rominger, T. Oeser, F. Hampel, A. Görling, M. Kivala, *Chem. Eur. J.* **2020**, *26*, 13157–13162.
- [5] T. A. Schaub, S. M. Brülls, P. O. Dral, F. Hampel, H. Maid, M. Kivala, *Chem. Eur. J.* **2017**, *23*, 6988–6992.
- [6] M. P. Duffy, W. Delaunay, P. A. Bouit, M. Hissler, *Chem. Soc. Rev.* **2016**, *45*, 5296–5310.
- [7] E. Regulska, C. Romero-Nieto, *Dalton Trans.* **2018**, *47*, 10344–10359.
- [8] a) S. Furukawa, Y. Suda, J. Kobayashi, T. Kawashima, T. Tada, S. Fujii, M. Kiguchi, M. Saito, *J. Am. Chem. Soc.* **2017**, *139*, 5787–5792; b) M. A. Shameem, A. Orthaber, *Chem. Eur. J.* **2016**, *22*, 10718–10735; c) P. Hindenberg, F. Rominger, C. Romero-Nieto, *Angew. Chem. Int. Ed.* **2021**, *60*, 766–773; *Angew. Chem.* **2021**, *133*, 777–785; d) G. Pfeifer, F. Chahdoura, M. Papke, M. Weber, R. Szucs, B. Geffroy, D. Tondelier, L. Nyulászi, M. Hissler, C. Müller, *Chem. Eur. J.* **2020**, *26*, 10534–10543.
- [9] a) J. A. L. Wells, M. A. Shameem, A. K. K. Gupta, A. Orthaber, *Inorg. Chem. Front.* **2020**, *7*, 4052–4061; b) J. P. Green, D. Morales Salazar, A. K. Gupta, A. Orthaber, *J. Org. Chem.* **2020**, *85*, 14619–14626; c) A. El Nahhas, M. A. Shameem, P. Chabera, J. Uhlig, A. Orthaber, *Chem. Eur. J.* **2017**, *23*, 5673–5677.
- [10] a) X. Pan, X. Wang, Y. Zhao, Y. Sui, X. Wang, *J. Am. Chem. Soc.* **2014**, *136*, 9834–9837; b) G. Tan, S. Li, S. Chen, Y. Sui, Y. Zhao, X. Wang, *J. Am. Chem. Soc.* **2016**, *138*, 6735–6738; c) R. S. Ghadwal, M. K. Sharma, D. Rottschäfer, S. Blomeyer, B. Neumann, G. Stammler, A. Hinz, M. van Gastel, *Chem. Commun.* **2019**, *55*, 10408–10411.
- [11] A. Decken, C. J. Carmalt, J. A. C. Clyburne, A. H. Cowley, *Inorg. Chem.* **1997**, *36*, 3741–3744.
- [12] H. Miyake, T. Sasamori, N. Tokitoh, *Angew. Chem. Int. Ed.* **2012**, *51*, 3458–3461; *Angew. Chem.* **2012**, *124*, 3514–3517.
- [13] Y. V. Svyaschenko, A. Orthaber, S. Ott, *Chem. Eur. J.* **2016**, *22*, 4247–4255.
- [14] Calculations show that the *cis*-isomer is thermodynamically favoured by ca. 9.1 kJ/mol.
- [15] This conformation is identified in the solid-state structure of **P3**, however poor crystal quality precludes further analysis.
- [16] H. Miyake, T. Sasamori, J. I. C. Wu, P. v. R. Schleyer, N. Tokitoh, *Chem. Commun.* **2012**, *48*, 11440–11442.
- [17] A. M. Borys, *Organometallics* **2023**, *42*, 182–196.

Manuscript received: February 20, 2023

Accepted manuscript online: March 27, 2023

Version of record online: April 25, 2023